Highlights

- A demand index quantifying the residual deformation ratio is defined.
- Near-fault ground motions are applied as input excitations.
- Effects of the damage-control core and its shifting path are studied.
- Empirical formulas of residual displacement ratio demand are developed.

Residual displacement ratio demand of oscillators representing HSSF-EDBs subjected to near-fault earthquake ground motions

Ke Ke[a, b], Wei Wang[c,*], Michael C.H. Yam[b,d], Lu Deng[a]

[a] *Hunan Provincial Key Laboratory on Damage Diagnosis for Engineering Structures, Hunan University, Changsha, China*

[b] *Department of Building and Real Estate, The Hong Kong Polytechnic University, Hong Kong, China*

[c] *State Key Laboratory of Disaster Reduction in Civil Engineering, Tongji University, Shanghai, China*

[d] *Chinese National Engineering Research Centre for Steel Construction (Hong Kong Branch), The Hong Kong Polytechnic University, Hong Kong, China*

Abstract: This research investigates the post-earthquake residual displacement ratio demand of high strength steel frames with energy dissipation bays (HSSF-EDBs) under near-fault earthquake ground motions. The study focuses on the ultimate stage of the structure where the HSS frame develops sufficient inelastic deformations. The nonlinear force-displacement behaviour of a HSSF-EDB is idealised by a classical trilinear kinematic model, and the idealised hysteretic behaviour is assigned to oscillators for representing the novel system. To facilitate performance-based seismic design of HSSF-EDBs, the post-earthquake residual displacement demand is related to the yield displacement characterising yielding of energy dissipation bays using the trilinear oscillator analogy, and a non-dimensional residual displacement ratio is proposed. A large number of inelastic spectral analyses of trilinear oscillators covering a reasonable spectrum of hysteretic parameters are performed to quantify the influence of the essential variables on the residual displacement ratio demand of the systems. The results show that the residual displacement ratio of trilinear oscillators representing HSSF-EDBs subjected to near-fault earthquake ground motions is affected by hysteretic parameters in various yielding stages. To offer a practical tool for estimating the residual displacement demand of HSSF-EDBs in the preliminary design phase, empirical formulas quantifying the post-earthquake residual displacement ratio demand of trilinear oscillators are proposed. Finally, the effectiveness of using trilinear oscillators for quantifying post-earthquake residual displacement demand of HSSF-EDBs is emphasised by a comparative study on seismic responses of a prototype HSSF-EDB system and equivalent oscillators under near-fault ground motion samples.

Keywords: High strength steel, Energy dissipation bay, Residual displacement ratio, Trilinear oscillator, Empirical formula.

---

* Corresponding author.

Email address: weiwang@tongji.edu.cn (W Wang)

1. Introduction

In order to achieve the life-safety objective, the widely used ductility-based seismic design philosophy aims to produce structures with sufficient ductility. In this context, structural elements (e.g. members and connections) in a conventional steel moment resisting frame (MRF) designed according to this philosophy may develop inelastic deformation in rapid succession when subjected to moderate to strong earthquake events. Although ductile performance and stable energy dissipation of conventional steel MRFs may enable survival of the system, seismic loss estimations and post-earthquake damage identifications indicate that inelastic actions of structural components may produce severe damages and residual deformations [1-3], and hence long occupancy suspension due to repair works or even complete demolition of the structure are expected, which become major concerns in modern seismic engineering. In general, the lessons from recent earthquake attacks signal the demand of more sustainable steel MRFs towards a higher level of seismic resistance, and new ways of enhancing seismic resilience [4-6] of steel MRFs with reduced post-earthquake residual deformations are actively pursued by the research community.

Among the recently emerged innovative concepts such as self-centring technology [7-13] and steel MRFs equipped with supplemental energy dissipation dampers [14, 15], interests have also been directed to the 'hybrid-steel-based' [16-18] or 'dual-steel-based' [19-22] steel MRFs. Specifically, a rational combination of sacrificial members or elements made of various steel grades enables modulation of nonlinear force-displacement response of a steel MRF. In particular, the damage-control behaviour [23-26] that locks inelastic actions

63 in target components can be realised in an expected deformation range, which is also
64 effective for mitigating post-earthquake residual deformations. For example, Charney and
65 Atlayan [17, 18] revealed the encouraging seismic performance of hybrid steel structures
66 based on numerical studies. Ke and Chen [24] proposed the notion of high strength steel
67 (HSS) frame with energy dissipation bays (HSSF-EDBs) as a typical dual-steel-based steel
68 MRF. The design concept of a HSSF-EDB is schematically illustrated in Fig. 1a. The
69 system is composed of a HSS main frame enhanced by energy dissipation bays with
70 energy dissipation beams. Under earthquake loadings, the inelastic actions are first
71 triggered and locked in the energy dissipation bays, while the HSS frame responds
72 elastically in a wide deformation range. Thus, the structure can restore close to its original
73 position owing to the elastic restoring force provided by the elastic HSS frame, and hence
74 the post-earthquake residual deformation of the system is mitigated. Nevertheless, the
75 recentring ability of a HSSF-EDB is greatly compromised after the system entering the
76 ultimate stage where the HSS frame develops significant yielding, and hence a pronounced
77 increase of residual deformation is expected due to the inelastic actions of structural
78 members. Therefore, to provide a more comprehensive interpretation of the post-
79 earthquake residual deformation demand of the HSSF-EDB system, particularly when a
80 structure progresses to the ultimate stage, more research efforts are required.

81 The present study focuses on the post-earthquake residual displacement responses of the
82 HSSF-EDBs in the ultimate stage, and the work also contributes to a practical model for
83 relating the structural hysteretic parameters with the post-earthquake residual displacement
84 of the systems. Recognising that near-fault earthquake ground motions with a pronounced

velocity pulse tend to import a large amount of energy into a structure in a short time, a HSSF-EDB may be exposed to higher risks of being pushed to the ultimate stage when subjected to this kind of seismic event. Hence, the focus of this work is to examine the residual displacement response of the HSSF-EDBs subjected to near-fault earthquake ground motions with evident velocity pulses. Firstly, the hysteretic behaviour of the HSSF-EDBs in the ultimate stage is reviewed, and the influential hysteretic parameters are clarified. Then, single-degree-of-freedom oscillators with a trilinear force-displacement hysteretic model validated by the previous experiment programme conducted by the first author and colleagues [24] are utilised for representing a HSSF-EDB structure. To facilitate performance-based seismic design of a HSSF-EDB, a non-dimensional quantity defined as the residual displacement ratio is proposed and examined in detail based on nonlinear response history analysis (NL-RHA) of oscillators. In the analyses, a large number of near-fault earthquake ground motion records are used as input excitations. Based on the analysis database, the effects of the essential parameters on the residual displacement ratio demand of trilinear oscillators representing HSSF-EDB in the ultimate stage are examined, and empirical expressions for prescribing the residual displacement ratio demand of the trilinear oscillators are proposed for practical applications. For clarity, it is noted that direct application of the oscillator analogy may be applicable to a low-to-medium rise HSSF-EDB structure [16, 25], and the effective mass of the fundamental vibration mode should be above 90% of the total mass of the structure. For systems appreciably influenced by multi-vibration modes, the trilinear oscillators can be used to prescribe the residual displacement demand of a ‘modal oscillator’, but the interaction

between the modal oscillators on the residual deformation of a tall HSSF-EDB is beyond the scope of this study. It is also worth noting that although the research community engaged in seismic engineering explored various multi-linear hysteretic models [27-31] including the trilinear hysteretic model [30, 31] in recent years, the emphases were generally given to force-displacement response and energy dissipation of the system, whereas the influence of the hysteretic parameters on the post-earthquake residual displacement demand of trilinear oscillators representing HSSF-EDBs has not been fully examined. For example, Guo and Christopoulos [31] developed a probability-based framework for estimating the post-earthquake residual displacement of trilinear oscillators, but the hysteretic parameters are not entirely applicable for representation of HSSF-EDBs. Therefore, it is believed that the current research work fills the knowledge gap in the field of the post-earthquake behaviour of trilinear oscillators representing HSSF-EDBs subjected to near-fault earthquakes.

2. Hysteretic behaviour and analytical model of HSSF-EDBs in the ultimate stage

2.1. Trilinear kinematic hysteretic model of HSSF-EDBs

When all the members in a HSSF-EDB structure develop sufficient inelastic deformation, the nonlinear force-displacement response of the system can be simplified by trilinear idealisation [24], as shown in Fig. 1b. In this study, to offer a better comprehension of the post-earthquake residual deformation demand of HSSF-EDBs progressing to the ultimate stage, single-degree-of-freedom (SDOF) systems assigned with the validated trilinear kinematic hysteretic model are utilised as analytical tools. In

particular, the roof displacement response and the base shear of a HSSF-EDB subjected to earthquake ground motions can be associated with the displacement and force indicator of the equivalent oscillator, as shown in Fig. 1a. The force versus displacement response of the representative oscillator [16, 32] is given as

$$F = \begin{cases} K\delta & 0 \le \delta \le \delta_{y1} \\ \alpha_1 K\delta + (1-\alpha_1)K\delta_{y1} & \delta_{y1} < \delta \le \delta_{y2} \\ \alpha_2 K\delta + (\alpha_1 - \alpha_2)K\delta_{y2} + (1-\alpha_1)K\delta_{y1} & \delta_{y2} < \delta \end{cases} \quad (1)$$

where K = elastic stiffness; δ = displacement of the equivalent oscillator; F = base shear of the equivalent oscillator; δ_{y1} = first yield displacement of the equivalent oscillator characterising yielding of the energy dissipation bays; δ_{y2} = second equivalent yield displacement of the equivalent oscillator characterising yielding of the HSS frame ($\zeta_1\delta_{y1}$); ζ_1 = yield displacement ratio (δ_{y2} / δ_{y1}); α_1 = post-yielding stiffness ratio of the 'damage-control core' [16, 24] (Fig. 1b) and α_2 = post-yielding stiffness ratio of the ultimate stage. The ductility of the system can then be defined by $\mu = \delta_m/\delta_{y1}$ (where δ_m is the maximum displacement of an equivalent oscillator subjected to earthquake motions). The characteristics of the force versus displacement response of the oscillator representing a HSSF-EDB under hysteretic loading scenarios can be described by a classical trilinear kinematic model, and the hysteretic behaviour of the system can be quantified using reference lines governing the loading-unloading-reloading paths, i.e. l_1~l_8 in Fig. 1b. For clarity, the equations for the reference lines are given in **Appendix A**. It should be noted that to further mitigate post-earthquake residual deformations of the structure, it is desirable to activate yielding of the energy dissipation bays during unloading, and hence the hysteretic parameters quantifying the shape of the 'damage-control core', i.e. α_1 and ζ_1,

should satisfy $\alpha_1(\zeta_1\text{-}1)>1$. In essence, the hysteretic response of the trilinear oscillator representing a HSSF-EDB structure progressing to the ultimate stage can be quantified by shifting the damage-control core prescribed by l_1, l_2, l_7 and l_8 along the reference lines l_3~l_6, as schematically shown in Fig. 1c and Fig. 1d, respectively. Thus, the cyclic response of the system in the ultimate stage is influenced by a set of hysteretic parameters that quantify the shape of the damage-control core (i.e. α_1 and ζ_1) and the shifting path (i.e. α_2 controlling the slope of l_3~l_6). More detailed information about the hysteretic model and the validation study can be found in [24].

2.2. Residual displacement ratio

The dynamic balance equation of a trilinear oscillator [32] which can represent a HSSF-EDB system is reproduced by

$$m\ddot{\delta} + c\dot{\delta} + F(\delta, \delta_{y1}, \zeta_1, \alpha_1, \alpha_2) = -m\ddot{\delta}_g \tag{2}$$

where m = lumped mass of the representative trilinear oscillator; c = damping coefficient of the trilinear oscillator; δ = displacement quantity of the trilinear oscillator; $\dot{\delta}$ = velocity quantity of the trilinear oscillator; $\ddot{\delta}$ = acceleration quantity of the trilinear oscillator; $\ddot{\delta}_g$ = acceleration history of an earthquake motion (i.e. a near-fault earthquake for the current study) and $F(\delta, \delta_{y1}, \zeta_1, \alpha_1, \alpha_2)$ = restoring force of the trilinear oscillator. The restoring force-displacement response is governed by the trilinear hysteretic model as mentioned above.

In practical design of a HSSF-EDB, the equivalent yield displacement of the trilinear oscillator quantifying the initiation of inelastic deformation of the energy dissipation bays

(i.e. δ_{y1}) is a critical index for conducting performance-based seismic design of HSSF-EDBs [16, 24]. Therefore, to facilitate seismic design of HSSF-EDBs, a non-dimensional index, i.e. the residual displacement ratio, correlating the post-earthquake residual deformation of the entire structure and the first yield displacement characterising yielding of the energy dissipation bays is proposed in this work. The residual displacement ratio of a trilinear oscillator representing the HSSF-EDB is given by

$$\eta=\left|\frac{\delta_r}{\delta_{y1}}\right| \tag{3}$$

where δ_r = post-earthquake residual displacement of the trilinear oscillator.

It is also worth pointing out that the realistic residual deformation indicators (e.g. residual interstorey drift) of a HSSF-EDB behaving as a multi-degree-of-freedom (MDOF) system are influenced by additional parameters such as interaction of multi-modes, structural arrangement and damage-evolution mode of the structure, which is not completely reflected by the post-earthquake residual displacement ratio of a trilinear oscillator. The influences of these factors can be further considered based on the residual displacement ratio of the trilinear oscillators, which is beyond the scope of this study.

3. Residual displacement ratio demand of trilinear oscillators representing HSSF-EDBs

3.1. Earthquake ground motions

To characterise the post-earthquake residual displacement ratio of trilinear oscillators representing HSSF-EDB structures under near-fault earthquakes, a database including one hundred (100) near-fault earthquake ground motion records [33] are used as seismic input

195 in the analyses. The ground motion database was constructed by Hatzigeorgiou [33, 34],
196 and the primary features of near-fault earthquakes including evident velocity pulse and
197 displacement pulse were adopted to characterise a near-fault earthquake motion. Note that
198 these acceleration records of the earthquakes were monitored by stations close to the fault
199 rupture (i.e. with a distance below 10 km), and hence these records may reasonably capture
200 the features of near-fault earthquake motions. The rationale of the ground motion database
201 and detailed information about the ground motion samples is discussed in the literature
202 [33].
203
204 *3.2. Analysis procedure and parameter spectrum*

205 To offer a better interpretation of the residual displacement ratio demand of the trilinear
206 oscillators representing the HSSF-EDB under near-fault ground motions and characterise
207 the influence of hysteretic parameters, NL-RHAs of oscillators assigned with various
208 hysteretic parameters are carried out. From the perspective of performance-based seismic
209 engineering, it is useful to interpret the nonlinear behaviour of HSSF-EDBs under various
210 deformation levels, and hence a constant-ductility-based analysis procedure [25] with
211 iterations is utilised when computing the residual displacement ratio. The step-by-step
212 analysis procedure to determine the residual displacement ratio is schematically shown in
213 Fig. 2. In general, after developing the parameter matrix and quantification of the
214 maximum elastic force of the correlated elastic oscillator subjected to the ground motion
215 (F_e) by history response analysis (Step 1-Step 3), iterations are initiated by running NL-
216 RHA of the inelastic oscillator with a trial yield strength of F_{y1} close to F_e, and the

corresponding trial yield displacement of δ_{y1} along with the hysteretic parameters, e.g. α_1 and ζ_1, is assigned to the oscillator. In the iterative process (Step 4), F_{y1} is decreased gradually (i.e. in a small percentage ΔV in each analysis), and the iteration can be terminated when the convergence criterion (Fig. 2) is achieved. In particular, the difference between the actual ductility defined by the ratio of the maximum displacement of the oscillator under a ground motion (δ_m) to δ_{y1} and the expected ductility (μ) should not be over μ/1000. Then, the nonlinear force versus displacement response history of the trilinear oscillator subjected to the ground motion can be finalised. Thus, δ_r can be extracted from the analysis database, and the residual displacement ratio can be calculated according to Eq. (3).

Previous research works [1, 16, 24, 35, 36] have shown that a large value of post-yielding stiffness ratio of the damage-control core (α_1) can result in further mitigation of post-earthquake residual deformations. For this reason, α_1 is varied from 0.5 to 0.9 with an increment of 0.1 in the analyses. The yield displacement ratio (ζ_1) quantifying the inelastic deformation range of damage-control core is increased from 4 to 10 with an increment of 1. Thus, the combinations of α_1 and ζ_1 can be used to represent various shapes of the damage-control core in practical cases. Comparatively, when the system progresses towards the ultimate stage, the post-yielding stiffness ratio in the ultimate stage (α_2) of a steel structure generally fluctuates in a relatively narrow spectrum. For the HSSF-EDBs, it should be noted that the post-yielding behaviour of the structure in the ultimate stage is greatly influenced by the post-yielding behaviour of HSS. However, recent research findings [37-39] indicate that the HSS does not exhibit sufficient post-yielding strain hardening as

239 observed in the tests of mild carbon steel, and the ratio of the ultimate strength to the yield
240 strength of the HSS is close to unity. In addition, after a structure reaching the ultimate
241 stage, the P-delta effect would become more pronounced, and hence the post-yielding
242 stiffness ratio of the structure can be further compromised [17, 18, 40]. Thus, in the present
243 study, relatively small post-yielding stiffness ratios in the ultimate stage (α_2) increasing
244 from 0 to 0.02 with an increment of 0.01 are included in the parameter matrix. To
245 investigate the influence of the maximum inelastic deformation, the ductility (μ) is
246 increased from 4.5 to 20 with an increment of 0.5. It is worth mentioning that the ductility
247 defined by the ratio of the expected maximum displacement to the equivalent yield
248 displacement characterising yielding of the energy dissipation bays actually quantifies the
249 ductility of the energy dissipation bays rather than the entire structure. To shed insightful
250 lights on the effect of the nonlinear quantities on the residual displacement ratio demand of
251 a trilinear oscillator, hysteretic parameters in the matrix (i.e. α_1, α_2, ζ_1 and μ) are
252 independent of each other in the analysis, but the ductility is always set larger than the
253 yield displacement ratio in each combination of hysteretic parameters. Also, since the main
254 focus of this study is on the residual displacement ratio demand of HSSF-EDBs, the
255 ductility capacity of the structure is not further explored. However, a reader may be aware
256 of the fact that HSS generally possesses limited ductility, and special care should be taken
257 to ensure the inelastic deformation capacity of the HSS frame in practical design. All the
258 hysteretic parameter combinations satisfy the precondition of $\alpha_1(\zeta_1\text{-}1) > 1$ [16, 24]. As the
259 emphasis of the study is given to multi-storey HSSF-EDBs which may be more cost-
260 effective from the perspective of resilient seismic engineering, the period of the oscillators

261 is varied from 0.5 s to 5 s covering a reasonable spectrum of multi-storey steel frame
262 structures. For instance, the lower limit of the fundamental vibration period of a three-
263 storey steel MRF with a storey height of 3.3 m is approximately 0.5 s according to [41]. In
264 all the analyses, the damping ratio (ξ) of 5% is assumed, which is applicable for steel
265 structures [6, 16, 24]. To capture the actual residual displacement of the oscillators after an
266 earthquake event, additional analysis time (i.e. 100 s) is employed in each analysis,
267 allowing decaying of the vibration of the system. In total, more than 12 million residual
268 displacement ratios (η) of oscillators are obtained.
269
270 **4. Analytical results and discussions**
271 *4.1. Effect of the damage-control core shape*
272 To clarify the effect of the shape of the damage-control core on the post-earthquake
273 residual displacement ratios of the trilinear oscillators representing the HSSF-EDB, the
274 effect of the post-yielding stiffness ratio of the damage-control core (α_1) and the yield
275 displacement ratio (ζ_1) on the residual displacement ratio demand is discussed in this
276 section. Representative mean η demands with various α_1 and ζ_1 are shown in Fig. 3. As can
277 be seen in Fig. 3a, although α_1 is a key parameter for minimising post-earthquake residual
278 deformations when the system is deformed in the damage-control core, it is observed that a
279 variation of α_1 does not produce a drastic change of the mean η demand regardless of the
280 variation of ζ_1 and μ, and negligible fluctuation of the η demand is characterised. However,
281 it should be re-emphasised that the post-residual displacement ratio is a normalised
282 quantity and does not directly quantify the absolute residual deformation of a structure. In

addition, this observation is also understandable since the post-earthquake residual displacement ratio of a trilinear oscillator representing HSSF-EDB progressing to the ultimate stage may be appreciably affected by the shift action of the damage-control core (Fig. 1c and Fig. 1d) rather than the post-yielding stiffness ratio of the damage-control core (α_1). In particular, after the structure is pushed to significant inelastic deformation with the damage-control core shifting away from the original position (Fig. 1c), the recentring behaviour of the structure strongly depends on the re-yielding of the HSS frame with the damage-control core shifting back (Fig. 1d). In contrast, Fig. 3b shows that with a specified μ, an increasing ζ_1 produces a pronounced reduction of the mean η demand due to the fact that the shift action of the damage-control core is suppressed in these cases.

In this context, with a given ductility, increasing ζ_1 (i.e. the inelastic deformation range of the damage-control core) is a promising alternative as it enhances the ability of the HSSF-EDB to restricting inelastic damages in the energy dissipation bays, and concurrently mitigates the shift action of the damage-control core. In practical engineering, the 'dual-steel' technology enables flexible modulation of the shape of the damage-control core, and a significant deformation range of the damage-control core can be ensured by enlarging the yield drift gap between the HSS frame and energy dissipation bays.

4.2. Effect of hysteretic parameters of the ultimate stage

As discussed above, the damage-control core shifts along the governing lines (i.e. l_3~l_6 in Fig. 1c and Fig. 1d) for a HSSF-EDBs system in the ultimate stage, and the post-yielding stiffness ratio of the ultimate stage (α_2) characterising the slope of the governing

lines and the ductility (μ) can be used to quantify the shift action of the damage-control core. To illustrate the effect of α_2 and μ on the residual displacement ratio of the oscillators representing HSSF-EDBs, representative mean η demand spectra for the trilinear oscillators with α_1=0.5 along with varied α_2, μ and ζ_1 are given in Fig. 4. In general, the residual displacement ratio may evidently increase with increase of μ. The representative results also indicate that when the prescribed μ is significant, increasing α_2 generally leads to decreasing mean η demand, but this trend is less evident in cases with smaller μ. Taking the cases with α_1 = 0.5 and ζ_1 = 8 as an example, it is observed that when α_2 is increased from 0 to 0.02, the mean η demand for the trilinear oscillator with the period of 1 s decreases by 18.5% when the prescribed μ is 20, whereas only a 5.5% decrease of the mean η demand is observed for the counterparts with μ=10.

Comparing the data points with various yield displacement ratio (ζ_1) describing the deformation range of the damage-control core, it is observed that α_2 also interacts with ζ_1 and affected the mean η demand. To reveal this effect, the representative results with varied ζ_1 are provided in Fig. 5. More specifically, representative results of cases with $\alpha_2 >$ 0 are plotted against the counterparts with α_2 = 0 as shown in the figure. The coordinate of the horizontal axis represents the mean η demand for cases with α_2 = 0, whereas the coordinate of the vertical axis is the mean η demand for cases with $\alpha_2 > 0$ (i.e. α_2 = 0.01 and α_2 = 0.02), and the other hysteretic parameters (i.e. α_1, ζ_1, and μ) are identical. According to Fig. 5, it is seen that data points generally cluster below the forty-five-degree line, showing that increasing α_2 is promising for reducing the post-earthquake residual displacement ratio demand, and this trend becomes more pronounced when ζ_1 is not

significant. It is worth pointing out that the results shown in Fig. 5 also echo the cascading effect between μ and α_2 on the mean η demand mentioned above since the data points with a larger μ tend to be farther away from the forty-five degree diagonal line. This observation demonstrates that the shifting path of the damage-control core is an essential factor affecting the residual displacement ratio of a HSSF-EDB in the ultimate stage. Increasing α_2 becomes effective for reducing post-earthquake residual displacement ratio when the HSS frame in the structure is expected to be experiencing severe inelastic actions under extreme earthquakes.

Nonetheless, it should be pointed out that the effect of the characteristics of the earthquake ground motion on the residual displacement ratio of inelastic systems may also be profound, and the observations from this study are based on the near-fault ground motion database (i.e. 100 ground motions). For the case of far-field earthquake motions [42] or other near-fault ground motion ensembles whose characteristics are different from the earthquake database used in this study, the residual displacement ratio demand of inelastic systems may or may not be identical to the observations drawn from this work. Thus, special caution should be taken when applying the findings from this work to those cases.

5. Design considerations

5.1. Empirical expressions of residual displacement ratio demand of trilinear oscillators representing HSSF-EDBs

From a practical application point of view, it is desirable to relate the mean residual

displacement ratio demand of trilinear oscillators representing HSSF-EDBs with the influential hysteretic parameters, and engineers can estimate the residual displacement ratio demand in structural design or evaluation procedures conveniently. To facilitate the direct application of the data pool, a set of preliminary empirical equations relating the mean residual displacement ratio demand to the influence of structural period and hysteretic parameters are developed using the nonlinear regression procedure. In particular, based on the database obtained from the inelastic spectral analyses in Section 4 (i.e. $4 \leq \zeta_1 \leq 10$, $4.5 \leq \mu \leq 20$, $0.5 \leq \alpha_1 \leq 0.9$ and $0 \leq \alpha_2 \leq 0.02$), the correlation among the mean residual displacement ratio demand (η), the structural period (T), and the ductility (μ) is regressed firstly. A trial-and-error procedure is utilised by applying linear equations, polynomials, rational equations, exponential equations and power equations to the residual displacement ratio database. Note that the regression procedure is conducted using the software TableCurve 3D [43], and the regressed equations are ranked by the coefficient of determination (R^2). The following equation is selected from more than 450 million built-in equations restored in the programme.

$$\eta = a + bT + cT^2 + dT^3 + f \ln \mu + g(\ln \mu)^2 \tag{4}$$

where a, b, c, d, f and g are regressed coefficients. Although the equation is developed based on curve fitting, the following relationship is satisfied.

$$\eta \overset{(\mu \to \infty)}{\to} \infty \tag{5}$$

This fundamental relationship is rational as the physical trend is captured, although it will not be realised in practical cases. Note that the format of the equation is finalised considering both practical simplicity and computational accuracy. Subsequently, the

effects of ζ_1 and α_2 are included in the empirical expressions. The following equations for quantifying the post-earthquake residual displacement ratio demand of trilinear oscillators are finalised using a trial-and-error procedure based on polynomials, given as follows:

$$a = a_1 + a_2\alpha_2 + a_3\alpha_2^2 \quad (6)$$

$$b = b_1 + b_2\alpha_2 + b_3\alpha_2^2 \quad (7)$$

$$c = c_1 + c_2\alpha_2 + c_3\alpha_2^2 \quad (8)$$

$$d = d_1 + d_2\alpha_2 + d_3\alpha_2^2 \quad (9)$$

$$f = f_1 + f_2\alpha_2 + f_3\alpha_2^2 \quad (10)$$

$$g = g_1 + g_2\alpha_2 + g_3\alpha_2^2 \quad (11)$$

where a_i, b_i, c_i, d_i, f_i and g_i (i=1, 2 and 3) are the regressed coefficients, and the coefficients for varied ζ_1 are indicated in Table 1. The convergence of the iterations is governed by the Pearson limit VII [33, 43]. In particular, the regressed coefficients are finalised when the following equation achieves the minimum, and this iterative procedure is performed by the programme.

$$\sigma = \sum[\ln(\sqrt{1 + (\eta_{\text{Exact}} - \eta_{\text{Model}})^2})] \quad (12)$$

where η_{Exact} = mean residual displacement ratio determined by the NL-RHAs of trilinear oscillators and η_{Model} = mean residual displacement ratio predicted by the proposed equations. To demonstrate the effectiveness of the developed empirical equations for predicting the mean residual displacement ratio demand of trilinear oscillators representing a HSSF-EDB structure subjected to the near-fault ground motions, η_{Model} for the trilinear oscillators with randomly selected hysteretic parameters falling in the parameter spectrum

393 are computed by the regressed equations and compared with the "exact" mean η demand
394 (η_{Exact}), as given in Fig. 6a. As can be seen, good agreement between the mean η demand
395 by NL-RHAs and the developed model (solid line and dash line in Fig. 6a) is obtained. To
396 have a more direct comprehension of the adequacy of the design model for quantifying the
397 post-earthquake residual displacement ratio demand of trilinear oscillators representing
398 HSSF-EDBs structures, all the mean η demands determined by NL-RHAs of trilinear
399 oscillators are plotted against the counterparts from the regressed model, as shown in Fig.
400 6b. It is observed that the data points are generally clustered close to the forty-five degree
401 diagonal line, and the maximum error of the regressed equations are generally within 10%,
402 except for cases with large ductility factors. These results strengthen the effectiveness of
403 the equations for prescribing the mean residual displacement ratio demand of trilinear
404 oscillators representing HSSF-EDBs.

405 However, it should be pointed out that since the design model is developed based on
406 data regression towards a practical tool in the preliminary design phase, the proposed
407 empirical equations and Table 1 are limited to the cases falling in the parameter matrix of
408 the current study. Importantly, the regressed coefficients are provided in Table 1 with each
409 case of ζ_1, and further simplifications (e.g. linear interpolation and polynomial
410 interpolation) are not recommended for other cases of ζ_1 which are not quantified in the
411 table, due to the fact that the parameter is varied with an increment of unity in the current
412 study. It is also of great significance to mention that the realistic residual displacement
413 ratio demand of a trilinear oscillator representing HSSF-EDB structures depends on the
414 feature of futural earthquake ground motions. Nonetheless, it is believed that the

examination of a large amount of near-fault ground motions with the classical averaging of the analysis data may reasonably capture the characteristics of the residual displacement ratio demand of trilinear oscillators under near-fault earthquake ground motions, which is in line with the previous research works [33, 34]. A reader should also be aware that the proposed empirical equations may not be applicable for predicting the residual displacement ratio demand of trilinear SDOF systems subjected to a single earthquake event or another earthquake ensemble whose characteristics are different from the database utilised in this work. In summary, the regression model proposed in the current work is for the purpose of preliminary design, and it is recommended to be used carefully depending on a designer's judgment.

5.2. Numerical examples and comments

In practical engineering, the residual displacement of an oscillator can be directly related to that of a low-to-medium rise HSSF-EDB structure. To demonstrate the ability of the trilinear oscillators for estimating post-earthquake residual deformations of low-to-medium rise HSSF-EDBs progressing into the ultimate stage, a case study on a prototype HSSF-EDB is carried out. Specifically, a three-storey HSSF-EDB is preliminarily designed according to the Chinese Code for Seismic Design of Buildings (GB 50011-2010) [44]. The basic acceleration is assumed to be 0.4 g, and the seismic weight is 2509 kN based on the assumed loading condition, i.e. a dead load of 4.8 kN/m^2 with the live load of 2.0 kN/m^2. The structural arrangement is shown in Fig. 7a. The energy dissipation bays are arranged at the external bays of the structure, and the sacrificial beams are designed with grade Q235 steel (yield strength = 235 MPa). The HSS frame is constructed by HSS Q460

steel (yield strength = 460 MPa). In the sacrificial beams, reduced beam sections are considered with 50% area reduction in the flanges [44, 45] to trigger the early yielding behaviour of the energy dissipation bays. The prototype structure is modelled by PERFORM-3D [46]. In the model, the force-deformation responses of the members are simplified by bilinear idealisation, and the detail information along with the rationale of the modelling techniques can be found in companion research works [16, 24] conducted by the first author and colleagues.

A pushover analysis of the three-storey structure is performed with the invariant lateral load in proportion to the fundamental vibration mode of the structure [47-49], and the base shear-roof drift response curve is shown in Fig. 7b along with the idealised trilinear response. NL-RHAs of the prototype system are also carried out with scaled near-fault ground motion samples randomly selected from the ensemble mentioned above, and the Rayleigh damping of 5% is assumed considering the first two vibration modes in the NL-RHAs. The representative roof displacement response histories under two scaled near-fault ground motions (i.e. records monitored by the station Cape Mendocino and Chi-Chi) are shown in Fig. 7c and Fig. 7d. To demonstrate the adequacy of using trilinear oscillators for representation of the structure, the seismic response of equivalent trilinear oscillator with the nonlinear dynamic properties of the fundamental vibration mode, i.e. mass (i.e. effective mass, period, nonlinear force-displacement characteristics and damping) are analysed with the earthquake ground motion inputs. Note that the displacement history response of the oscillators (u) can be converted to the predicted roof displacement [47-49] of the structure (Δ_r) using the equivalent oscillator analogy, i.e. $\Delta_r=\varphi_r\Gamma_1 u$, where φ_r = roof

element in the fundamental modal shape vector and Γ_1 is the modal participation factor of the fundamental mode. The converted responses are compared with the actual roof displacement of the structure subjected to earthquakes, as shown in Fig. 7c and Fig. 7d. As can be seen, reasonable agreement between the roof displacement responses of the three-storey HSSF-EDB and those determined by the equivalent trilinear oscillator is obtained, echoing research findings in a previous work [48]. Concurrently, the force-displacement responses of the oscillators subjected to ground motions are also given in the figures, and the shift of the damage-control core can be observed. For the purpose of comparison, the pushover response curve of the HSSF-EDBs is also idealised by the bilinear simplification [50] (Fig. 7b), which is widely used in current seismic design provisions. The roof displacement history of the prototype structure is also predicted using the oscillators assigned with the idealised bilinear force-displacement nonlinearity, and the converted responses are shown in Fig. 7c and Fig. 7d. According to the comparison, although the bilinear oscillators can reasonably quantify the peak roof displacement of the structure according to the "equal displacement rule" [48], they fail to prescribe the post-earthquake residual displacement response, and hence the necessity of using trilinear oscillators for quantifying the residual displacement demand of HSSF-EDBs structures is highlighted again.

6. Conclusions

The present paper contributes towards a comprehensive interpretation of the post-earthquake residual displacement ratio demand of the high strength steel frames equipped with energy dissipation bays (HSSF-EDBs) subjected to near-fault earthquake ground

motions, and the emphases are given to the ultimate stage of the system where all the members developed sufficient inelastic deformations. In this study, trilinear oscillators following the trilinear kinematic hysteretic law is used to represent HSSF-EDBs, and the residual displacement ratio defined by the post-earthquake residual displacement of the system to the displacement characterising yielding of the energy dissipation bays is utilised to prescribe the residual displacement demand of the novel systems, which is helpful to form a better understanding of the system from the perspective of performance-based seismic design. The influence of the hysteretic parameters on the post-earthquake residual displacement ratio of the systems is carefully examined based on more than 12 million inelastic spectral analyses of single-degree-of-freedom oscillators. The following observations can be drawn from the current study:

1. For a trilinear oscillator representing a HSSF-EDB in the ultimate stage with a specified ductility (μ), the variation of the post-yielding stiffness ratio of the damage-control core (α_1) does not lead to evident fluctuation of the mean residual displacement ratio demand (η). In contrast, an increasing yield displacement ratio (ζ_1), results in a pronounced decrease of the mean η demand.
2. The mean η demand increases with increasing μ, whereas an increasing post-yielding stiffness ratio in the ultimate stage (α_2) generally leads to the reduction of the residual displacement ratio of the system, particularly in cases where the expected μ is significant. However, in cases where μ is insignificant, the influence of α_2 on the mean η demand is less pronounced. Concurrently, the cascading effect between α_2 and ζ_1 on the post-earthquake residual displacement ratio of trilinear oscillators is also

505 characterised. In contrast, the contribution of increasing α_2 for mitigating the post-
506 earthquake residual displacement ratio demand of the trilinear oscillators becomes
507 less evident when ζ_1 is significant since in these cases the residual displacement ratio
508 demand would be dominated by the damage-control core, echoing the previous
509 finding.

510 3. Empirical formulas of the mean residual displacement ratio for the trilinear oscillators
511 subjected to near-fault earthquake ground motions are proposed using nonlinear
512 regression analysis based on the data pool of the post-earthquake residual
513 displacement ratio of trilinear oscillators, and practitioners can use the developed
514 empirical equations to prescribe the residual displacement ratio demand of HSSF-
515 EDBs in performance-based seismic design and evaluation procedures as a practical
516 start point.

517 It is re-emphasised that the research findings of the present research are based on single-
518 degree-of-freedom (SDOF) analogy, and hence the direct application of the research
519 findings in a HSS-EDB is valid for low-to-medium rise systems governed by the
520 fundamental vibration mode. However, as the seismic behaviour of multi-mode-sensitive
521 structures can be reasonably quantified with appropriate combination of responses of
522 modal oscillators, the developed data pool just offers a basis for further investigations of
523 residual deformation demands of taller HSSF-EDBs that are appreciably affected by multi-
524 modes. It is also worth noting that the post-earthquake residual displacement ratio is a
525 normalised quantity, and hence the physical essence may not be fully reflected by the
526 single indicator. To overcome this limitation, a multi-demand-indices-based design

527 methodology may be in need with additional demand quantities. In addition, a probability-
528 based design model considering a wider spectrum of parameters and various types of
529 earthquake ground motions is also in need. These works are currently being conducted by
530 the authors.

531

532 **Appendix A**

533 The trilinear kinematic hysteretic model described in Fig. 1 [16, 24, 32] follows the
534 classical trilinear kinematic law and can be used to describe the HSSF-EDB showing
535 multiple yielding stages. The cyclic force-displacement response of a HSSF-EDB system
536 entering the ultimate stage where the HSS frame developed sufficient yielding can be
537 idealised by multi-linear idealisation [32], and the equations are reproduced as follows:

538 $$F = \alpha_1 K\delta + (1-\alpha_1)K\delta_{y1} \quad \text{for } l_1 \quad \text{(A.1)}$$

539 $$F = \alpha_1 K\delta - (1-\alpha_1)K\delta_{y1} \quad \text{for } l_2 \quad \text{(A.2)}$$

540 $$F = \alpha_2 K\delta + (\alpha_1 - \alpha_2)K\delta_{y2} + (1-\alpha_1)K\delta_{y1} \quad \text{for } l_3 \quad \text{(A.3)}$$

541 $$F = \alpha_2 K\delta + (\alpha_1 - \alpha_2)K(\delta_{y2} - 2\delta_{y1}) + (\alpha_1 - 1)K\delta_{y1} \quad \text{for } l_4 \quad \text{(A.4)}$$

542 $$F = \alpha_2 K\delta - (\alpha_2 - \alpha_1)K(\delta_{y2} - 2\delta_{y1}) - (\alpha_1 - 1)K\delta_{y1} \quad \text{for } l_5 \quad \text{(A.5)}$$

543 $$F = \alpha_2 K\delta - (\alpha_1 - \alpha_2)K\delta_{y2} - (1-\alpha_1)K\delta_{y1} \quad \text{for } l_6 \quad \text{(A.6)}$$

544 $$F = K\delta + K(\delta_{y2} - \delta_{y1}) - \alpha_1 K(\delta_{y2} - \delta_{y1}) \quad \text{for } l_7 \quad \text{(A.7)}$$

545 $$F = K\delta - K(\delta_{y2} - \delta_{y1}) + \alpha_1 K(\delta_{y2} - \delta_{y1}) \quad \text{for } l_8 \quad \text{(A.8)}$$

546 For a HSSF-EDBs system experiencing earthquakes, the actual hysteretic response of
547 the system also depends on the earthquake ground motion histories.

548

Acknowledgements

This research is financially supported by the National Natural Science Foundation of China (Grant No. 51708197, 51778459 and 51890902). Funding support received from the Chinese National Engineering Research Centre for Steel Connection, The Hong Kong Polytechnic University (Project No. 1-BBV4) for the study is also gratefully acknowledged. The assistance of Miss Qingyang Zhao and Mr Wuhua Xie in this work is gratefully acknowledged.

References

[1] Macrae G, Kawashima K. Post-earthquake residual displacements of bilinear oscillators. Earthq Eng Struct Dyn 1997; 26(7): 701-716.

[2] Erochko J, Christopoulos C, Tremblay R, Choi H. Residual drift response of SMRFs and BRB frames in steel buildings designed according to ASCE 7-05. J Struct Eng 2011; 137(5): 589-599.

[3] Baiguera M, Vasdravellis G, Karavasilis TL. Dual seismic-resistant steel frame with high post-yield stiffness energy-dissipative braces for residual drift reduction. J Constr Steel Res 2016; 122: 198-212.

[4] Bruneau M, Chang SE, Eguchi RT, Lee GC, O'Rourke TD, Reinhorn AM, Shinozuka M, Tierney K, Wallace WA, Winterfeldt DV. A framework to quantitatively assess and enhance the seismic resilience of communities. Earthq spectra 2003; 19(4): 733-752.

[5] Cimellaro GP, Bruneau M. RAM. Framework for analytical qualification of disaster resilience. Eng Struct 2010; 32(11): 3639-3649.

[6] Pekcan G, Itani AM, Linke C. Enhancing seismic resilience using truss girder frame systems with supplemental devices. J Constr Steel Res 2014; 94: 23-32.

574 [7] Bruce TL, Eatherton MR. Behavior of post-tensioning strand systems subjected to
575 inelastic cyclic loading. J Struct Eng 2016; 142(10): 04016067.
576 [8] Wang W, Fang C, Liu J. Self-Centering beam-to-column connections with combined
577 superelastic SMA bolts and steel angles. J Struct Eng 2016; 143(2): 175.
578 [9] Wang W, Kong J, Zhang Y, Chu G, Chen Y. Seismic behavior of self-centering
579 modular panel with slit steel plate shear walls: experimental testing. J Struct Eng
580 2018; 144(1):04017179.
581 [10] Fang C, Wang W, He C, Chen Y. Self-centring behaviour of steel and steel-concrete
582 composite connections equipped with NiTi SMA bolts. Eng Struct 2017; 150:390-408.
583 [11] Wang W, Fang C, Yang X, Chen Y, Ricles J, Sause R. Innovative use of a shape
584 memory alloy ring spring system for self-centering connections. Eng Struct 2017; 153:
585 503-515.
586 [12] Wang W, Du X, Zhang Y, Chen Y. Experimental investigation of beam-through steel
587 frames with self-centering modular panels. J Struct Eng 2017; 143(5): 04017006.
588 [13] Hou H, Li H, Qiu C, Zhang Y. Effect of hysteretic properties of SMAs on seismic
589 behavior of self-centering concentrically braced frames. Struct Control Hlth 2017;
590 25(11): e2110.
591 [14] Qu B, Liu X, Hou H, Qiu C, Hu D. Testing of buckling-restrained braces with
592 replaceable steel angle fuses. J Struct Eng 2018; 144(3): 04018001.
593 [15] Symans MD, Charney FA, Whittaker AS, Constantinou MC, Kircher CA, Johnson
594 MW, Mcnamara RJ. Energy dissipation systems for seismic applications: current
595 practice and recent developments. J Struct Eng 2008; 134(1): 3-21.
596 [16] Ke K, Yam MCH. A performance-based damage-control design procedure of hybrid
597 steel MRFs with EDBs. J Constr Steel Res 2018; 143: 46-61.
598 [17] Charney FA, Atlayan O. Hybrid moment-resisting steel frames. Eng J AISC. 2011;

599 48(3): 169-182.
600 [18] Atlayan O, Charney FA. Hybrid buckling-restrained braced frames. J Constr Steel Res
601 2014; 96: 95-105.
602 [19] Dubina D, Stratan A, Dinu F. Dual high-strength steel eccentrically braced frames
603 with removable links. Earthq Eng Struct Dyn 2008; 37(15): 1703-1720.
604 [20] Tenchini A, D'Aniello M, Rebelo C, Landolfo R, Da Silva LS, Lima L. Seismic
605 performance of dual-steel moment resisting frames. J Constr Steel Res 2014; 101:
606 437-454.
607 [21] Tenchini A, D'Aniello M, Rebelo C, Landolfo R, da Silva LS, Lima L. High strength
608 steel in chevron concentrically braced frames designed according to Eurocode 8. Eng
609 Struct 2016; 124: 167-185.
610 [22] Wang F, Su M, Hong M, Guo Y, Li S. Cyclic behaviour of Y-shaped eccentrically
611 braced frames fabricated with high-strength steel composite. J Constr Steel Res 2016;
612 120: 176–187.
613 [23] Connor JJ, Wada A, Iwata M, Huang Y. Damage-controlled structures. I: Preliminary
614 design methodology for seismically active regions. J Struct Eng 1997; 123(4): 423-
615 431.
616 [24] Ke K, Chen Y. Seismic performance of MRFs with high strength steel main frames
617 and EDBs. J Constr Steel Res 2016; 126: 214-228.
618 [25] Ke K, Yam MCH, Ke S. A dual-energy-demand-indices-based evaluation procedure
619 of damage-control frame structures with energy dissipation fuses. Soil Dyn Earthq
620 Eng 2017; 95: 61-82.
621 [26] Ke K, Yam MCH, Deng L, Zhao Q. A modified DEB procedure for estimating
622 seismic demands of multi-mode-sensitive damage-control HSSF-EDBs. J Constr Steel
623 Res 2018; 150: 329-345.

624 [27] Macillo V, Shakeel S, Fiorino L, Landolfo R, Development and calibration of a
625 hysteretic model for CFS strap braced stud walls. Adv Steel Constr 2018; 14(3): 337-
626 360.
627 [28] Christopoulos C, Filiatrault A, Folz B. Seismic response of self-centring hysteretic
628 SDOF systems. Earthq Eng Struct Dyn 2002; 31(5): 1131-1150.
629 [29] Li G, Fahnestock L A. Seismic response of single-degree-of-freedom systems
630 representing low-ductility steel concentrically braced frames with reserve capacity. J
631 Struct Eng 2012; 139(2): 199-211.
632 [30] Guo J WW, Christopoulos C. Performance spectra based method for the seismic
633 design of structures equipped with passive supplemental damping systems. Earthq Eng
634 Struct Dyn 2013; 42(6): 935-952.
635 [31] Guo JWW, Christopoulos C. A probabilistic framework for estimating the residual
636 drift of idealized SDOF systems of non-degrading conventional and damped structures.
637 Earthq Eng Struct Dyn 2018; 47(2): 479-496.
638 [32] Ke K, Zhao Q, Yam MCH, Ke S. Energy factors of trilinear SDOF systems
639 representing damage-control buildings with energy dissipation fuses subjected to near-
640 fault earthquakes. Soil Dyn Earthq Eng 2018; 107:20-34.
641 [33] Hatzigeorgiou GD. Ductility demand spectra for multiple near-and far-fault
642 earthquakes. Soil Dyn Earthq Eng 2010; 30(4): 170-183.
643 [34] Hatzigeorgiou GD. Behavior factors for nonlinear structures subjected to multiple
644 near-fault earthquakes. Comput Struct 2010; 88(5): 309-321.
645 [35] Kawashima K, MacRae GA, Hoshikuma JI, Nagaya K. Residual displacement
646 response spectrum. J Struct Eng 1998; 124: 523-530.
647 [36] Nakashima M, Saburi K, Tsuji B. Energy Input and dissipation behaviour of
648 structures with hysteretic dampers. Earthq Eng Struct Dyn 1996; 25(5): 483–496.

649 [37] Xiang P, Jia LJ, Ke K, Chen Y, Ge H. Ductile cracking simulation of uncracked high
650 strength steel using an energy approach. J Constr Steel Res 2017; 138: 117-130.
651 [38] Wang YB, Li GQ, Cui W, Chen SW, Sun FF. Experimental investigation and
652 modeling of cyclic behavior of high strength steel. J Constr Steel Res 2015; 104: 37-
653 48.
654 [39] Ke K, Xiong YH, Yam MCH, Lam ACC, Chung KF. Shear lag effect on ultimate
655 tensile capacity of high strength steel angles. J Constr Steel Res 2018; 145:300-314.
656 [40] Gupta A, Krawinkler H. Behavior of ductile SMRFs at various seismic hazard levels.
657 J Struct Eng 2000; 126(1): 98-107.
658 [41] Goel RK, Chopra A K. Period formulas for moment-resisting frame buildings. J
659 Struct Eng 1997; 123(11): 1454-1461.
660 [42] Chopra AK, Chintanapakdee C. Comparing response of SDF systems to near-fault
661 and far-fault earthquake motions in the context of spectral regions. Earthq Eng Struct
662 Dyn 2001; 30(12): 1769-1789.
663 [43] Jandel Scientific Software. TableCurve 3D Automated Surface Fitting Software.
664 Jandel Sci; 1993.
665 [44] CMC. Code for Seismic Design of Buildings (GB 50011-2010). China Ministry of
666 Construction: Beijing, 2010.
667 [45] AISC. Prequalified Connections for Special and Intermediate Steel Moment Frames
668 for Seismic Applications, ANSI/AISC 358-05. American Institute for Steel
669 Construction: Chicago, 2005.
670 [46] CSI. PERFORM-3D v4.0.3 nonlinear analysis and performance assessment for 3D
671 structures. California, USA: Computers and Structures Inc.; 2006.
672 [47] Chopra AK, Goel RK. A modal pushover analysis procedure for estimating seismic
673 demands for buildings. Earthq Eng Struct Dyn 2002; 31(3): 561-582.

674 [48] Leelataviwat S, Saewon W, Goel SC. Application of energy balance concept in
675 seismic evaluation of structures. J Struct Eng 2009; 135: 113-121.
676 [49] Chopra AK, Goel RK, Chintanapakdee C. Evaluation of a modified MPA Procedure
677 assuming higher modes as elastic to estimate seismic demands. Earthq Spectra 2004;
678 20(3): 757-778.
679 [50] FEMA. Pre-standard and commentary for the seismic rehabilitation of buildings,
680 report FEMA-356. Washington, DC: SAC Joint Venture for the Federal Emergency
681 Management Agency; 2000.

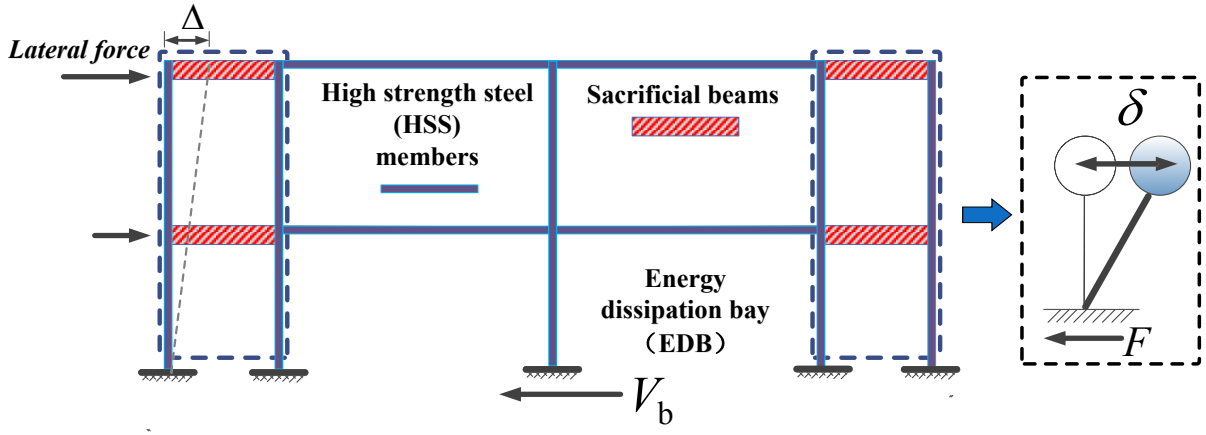

(a)

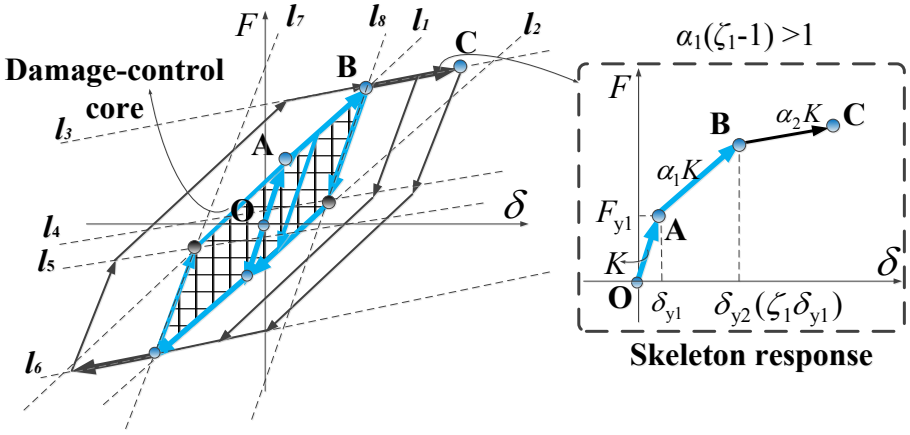

(b)

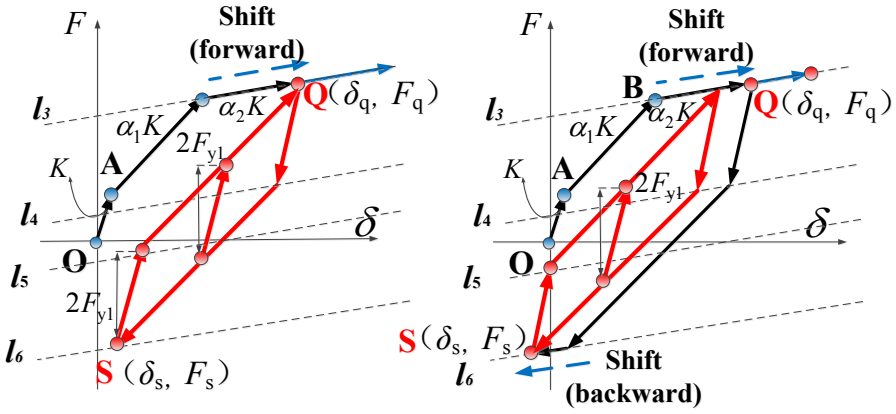

(c) (d)

Fig. 1 Concept of HSSF-EDBs and hysteretic behaviour: (a) concept of the system and single-degree-of-freedom analogy, (b) trilinear kinematic model, (c) shift of the damage-control core (forward) and (d) shift of the damage-control core (forward and backward).

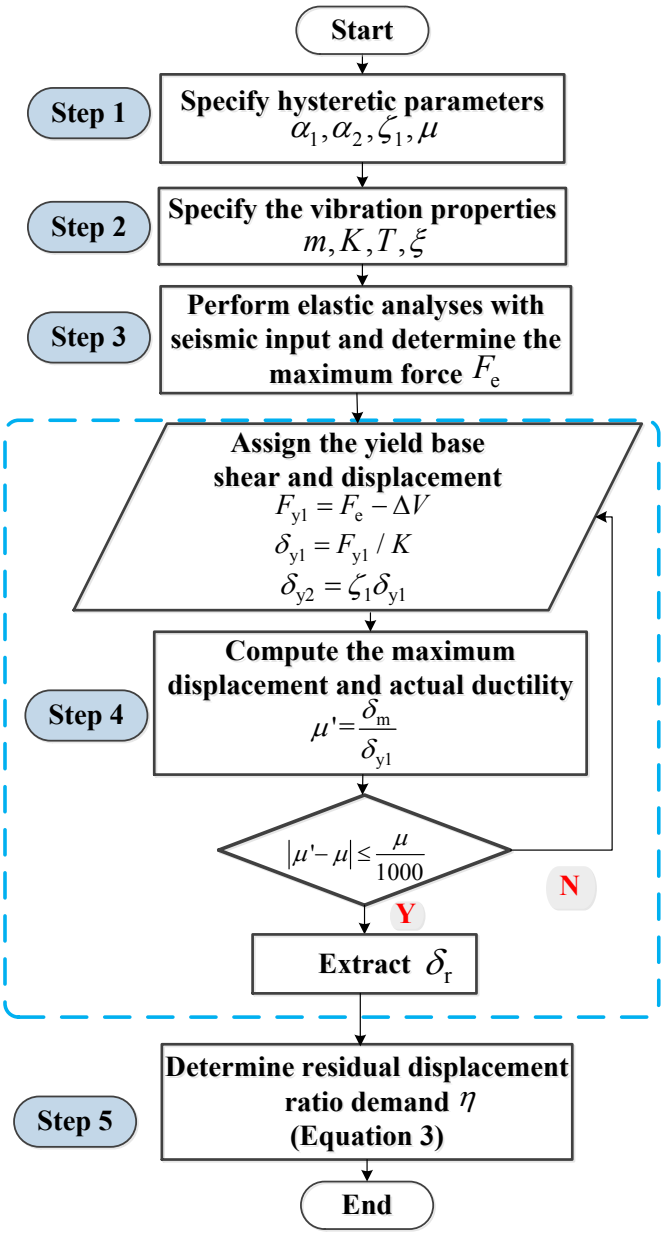

Fig. 2 Step-by-step procedure for determining the residual displacement ratio.

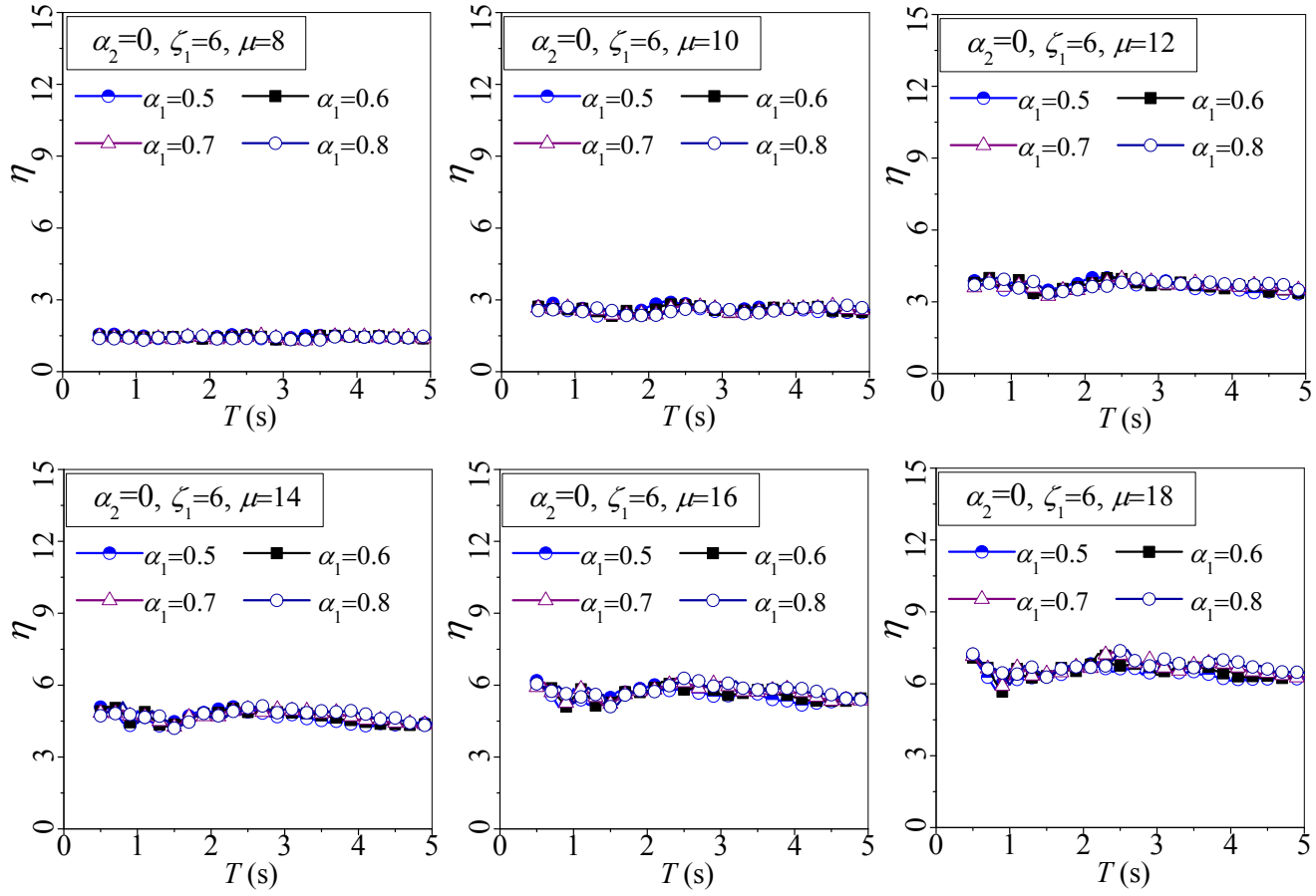

(a)

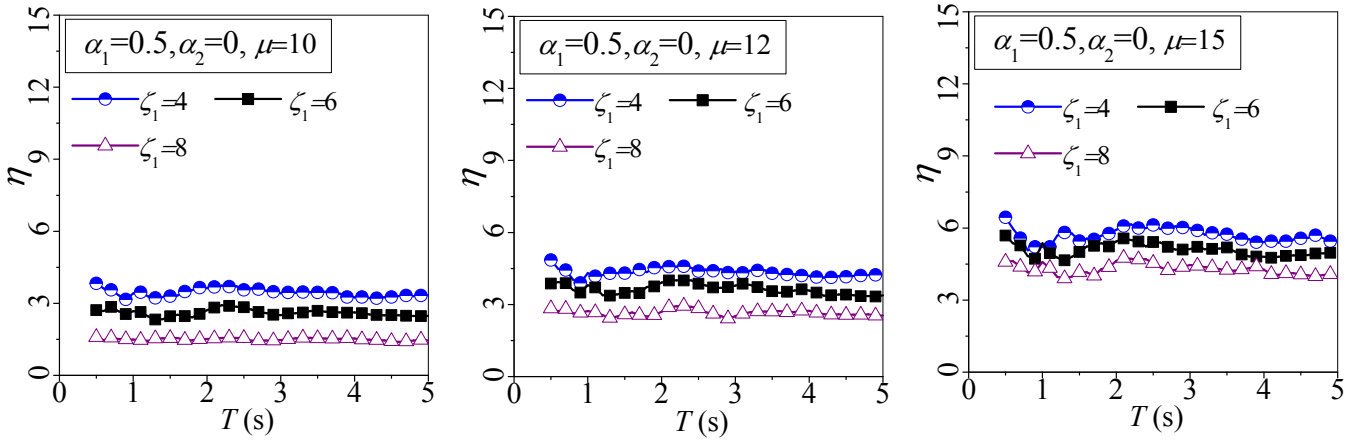

(b)

Fig. 3 Effect of the shape of the damage-control core: (a) effect of α_1 and (b) effect of ζ_1.

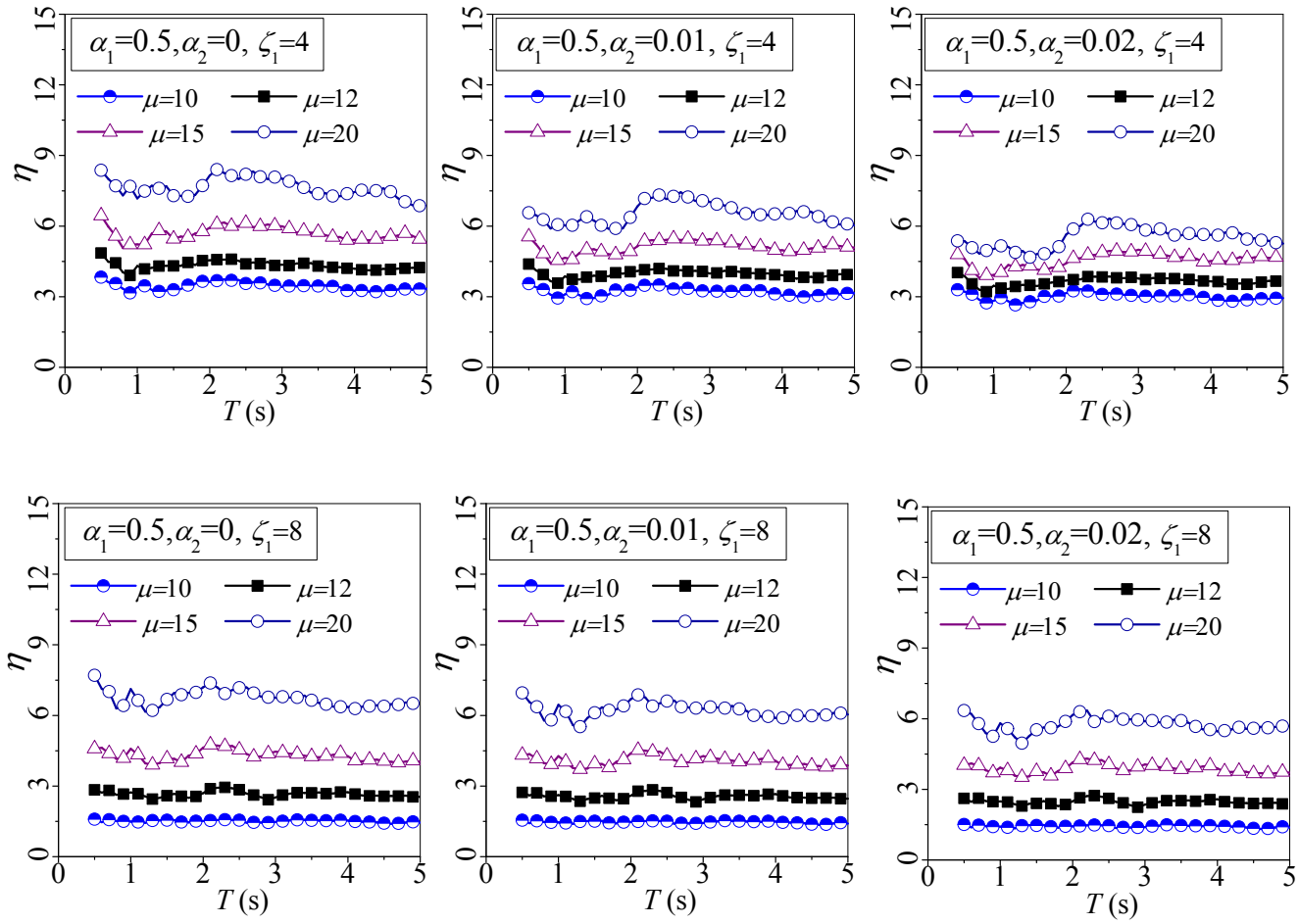

Fig. 4 Effect of the ductility (μ) and the post-yielding stiffness ratio in the ultimate stage (α_2).

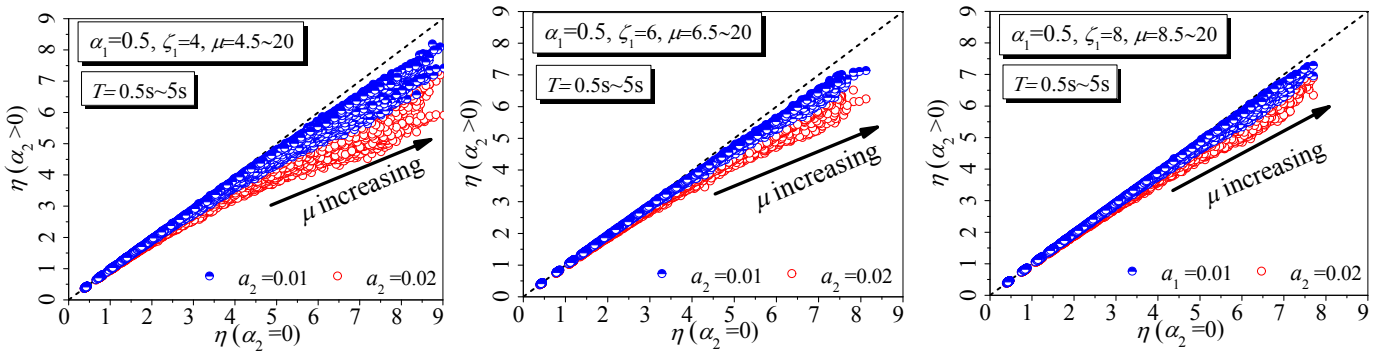

Fig. 5 Cascading effect of the post-yielding stiffness ratio in the ultimate stage (α_2) and the yield displacement ratio (ζ_1).

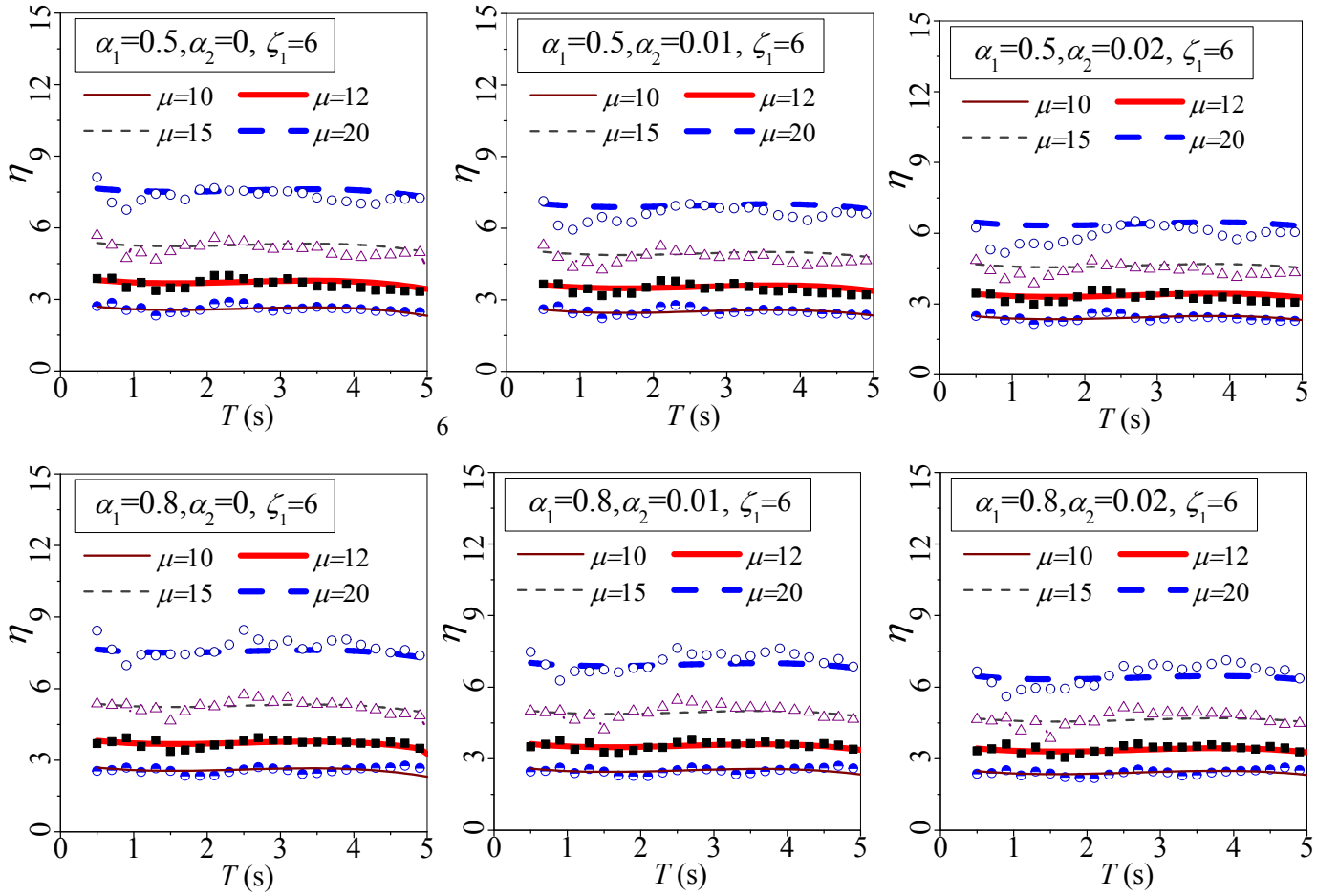
α1=0.5,α2=0, ζ1=6
α1=0.5,α2=0.01, ζ1=6
α1=0.5,α2=0.02, ζ1=6
α1=0.8,α2=0, ζ1=6
α1=0.8,α2=0.01, ζ1=6
α1=0.8,α2=0.02, ζ1=6
μ=10
μ=12
μ=15
μ=20
η
T (s)

(a)

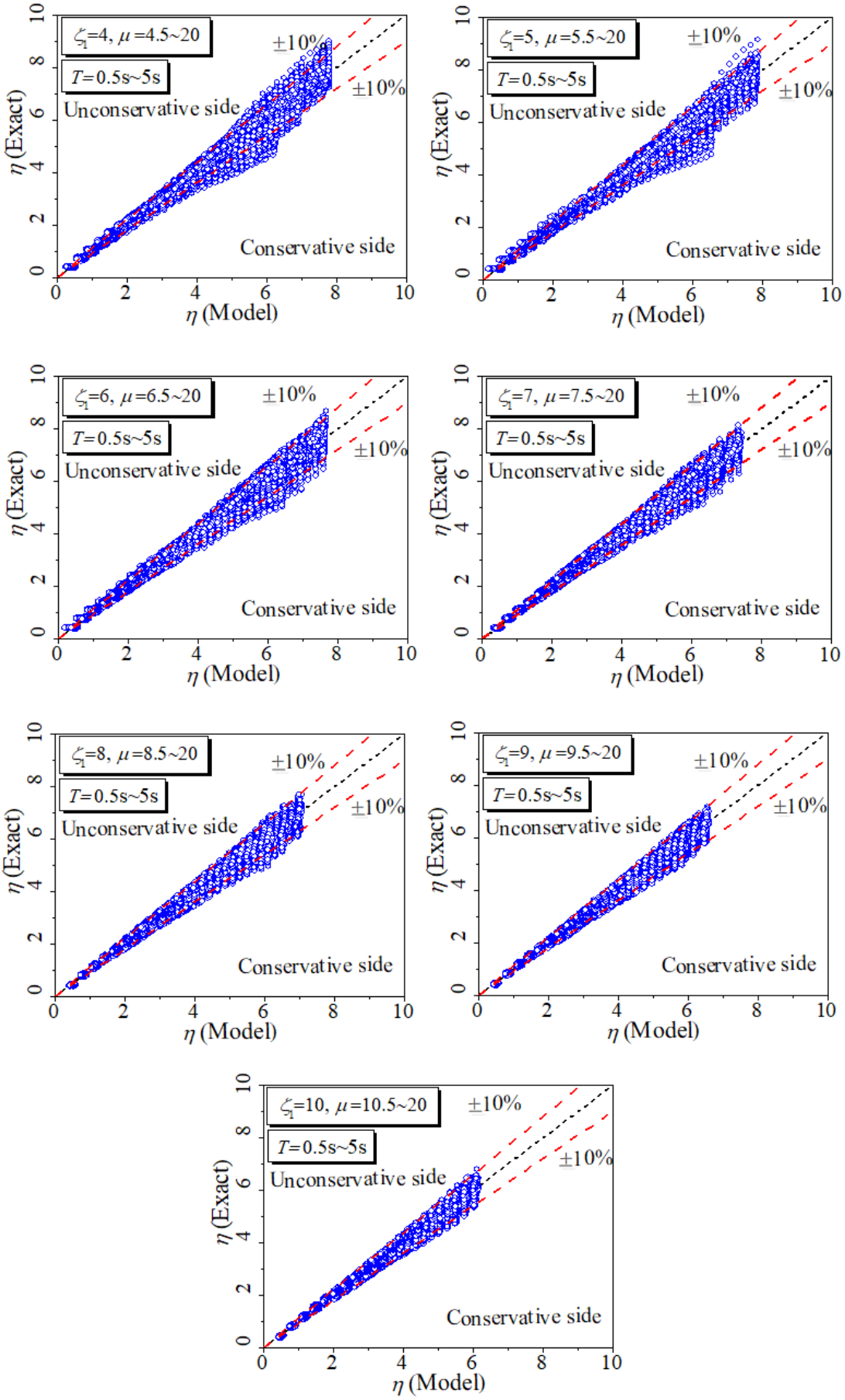

(b)

Fig. 6 Comparison of residual displacement ratio demand from the developed equations and NL-RHAs of the oscillators: (a) comparison of mean η demand spectra (randomly selected) and (b) comparison of data points.

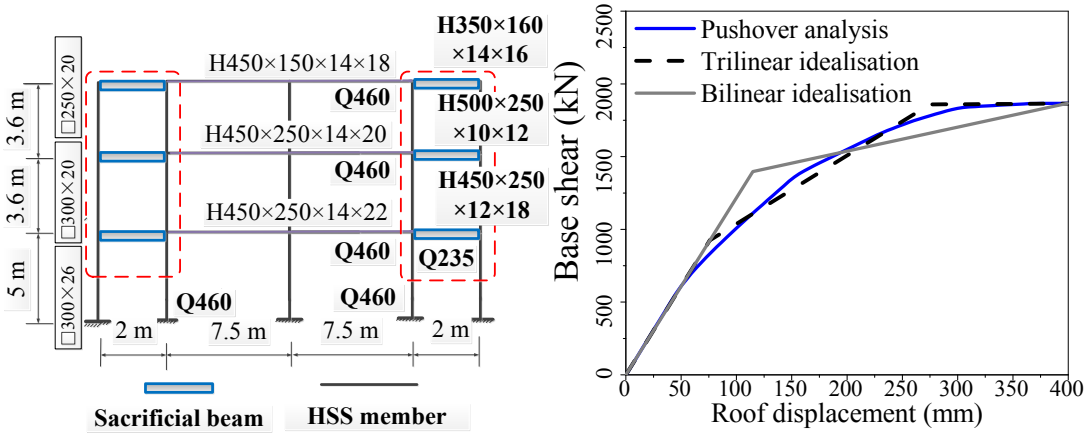

(a) (b)

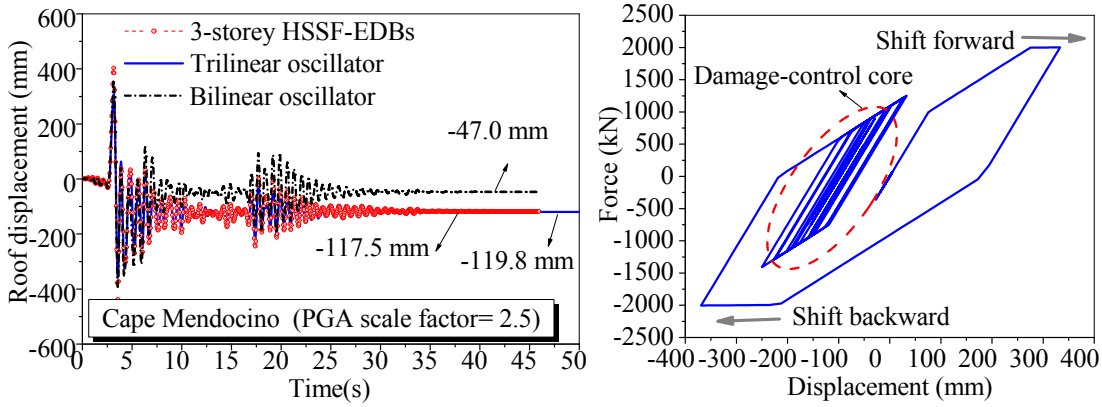

(c)

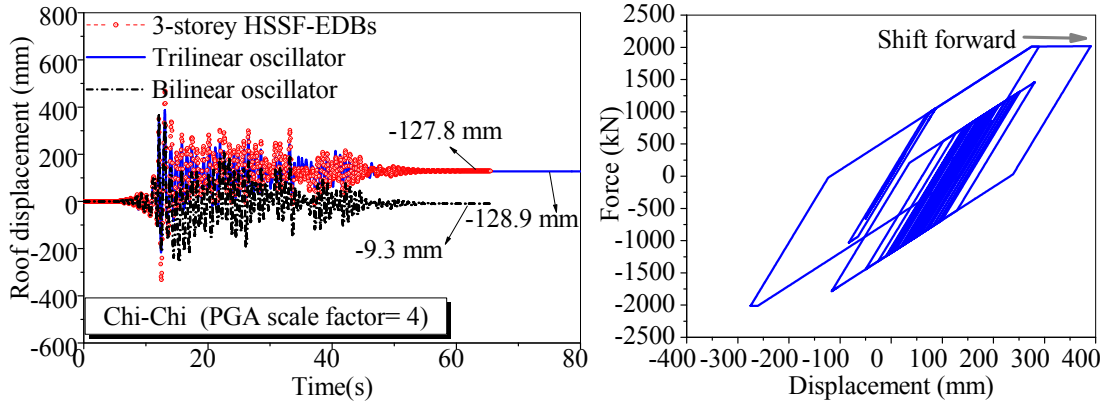

(d)

Fig. 7 Numerical example of a HSSF-EDB and equivalent oscillators: (a) arrangement of a prototype structure, (b) pushover response of the prototype structure and idealised response, (c) seismic response under Cape Mendocino ground motion and (d) seismic response under Chi-Chi ground motion.

Table 1 Regressed coefficients a_i, b_i, c_i, d_i, f_i and g_i (i=1~3) for the empirical expressions

Yield displacement ratio	**Coefficient（i=1,2 and 3）**	**a_i, b_i, c_i, d_i, f_i and g_i**					
		a_i	b_i	c_i	d_i	f_i	g_i
Case ζ_1=4	i=1	**0.18**	**-0.47**	**0.22**	**-0.03**	**-1.58**	**1.43**
	i=2	**-105.77**	**-10.75**	**5.80**	**-0.73**	**132.46**	**-41.61**
	i=3	**904.70**	**744.68**	**-404.25**	**54.65**	**-1230.00**	**343.40**
Case ζ_1=5	i=1	**0.25**	**-0.54**	**0.26**	**-0.03**	**-2.74**	**1.79**
	i=2	**127.40**	**-10.22**	**4.36**	**-0.39**	**150.98**	**-44.42**
	i=3	**-771.50**	**691.15**	**-313.96**	**37.13**	**268.50**	**49.00**
Case ζ_1=6	i=1	**-0.15**	**-0.51**	**0.24**	**-0.03**	**-3.16**	**1.94**
	i=2	**-201.60**	**1.96**	**-1.78**	**0.41**	**206.68**	**-53.94**
	i=3	**1789.50**	**50.92**	**-1.93**	**-3.33**	**-1709.30**	**403.57**
Case ζ_1=7	i=1	**0.09**	**-0.42**	**0.18**	**-0.02**	**-4.14**	**2.22**
	i=2	**-244.20**	**-3.50**	**1.15**	**-0.05**	**237.91**	**-58.33**
	i=3	**1053.00**	**216.70**	**-83.23**	**8.28**	**-1460.40**	**338.20**
Case ζ_1=8	i=1	**0.14**	**-0.37**	**0.16**	**-0.02**	**-4.71**	**2.39**
	i=2	**-308.98**	**-2.05**	**0.85**	**-0.07**	**282.04**	**-64.67**
	i=3	**2934.20**	**85.75**	**-28.50**	**2.35**	**-2473.50**	**508.35**
Case ζ_1=9	i=1	**-2.43**	**-0.36**	**0.15**	**-0.02**	**-3.62**	**2.23**
	i=2	**-165.10**	**0.40**	**-0.18**	**0.04**	**157.44**	**-37.69**
	i=3	**-3058.80**	**29.75**	**-5.50**	**-0.26**	**2424.00**	**-480.00**
Case ζ_1=10	i=1	**-4.99**	**-0.35**	**0.14**	**-0.02**	**-2.44**	**2.07**
	i=2	**-357.75**	**2.75**	**-1.18**	**0.16**	**303.55**	**-65.13**
	i=3	**5621.00**	**-120.55**	**-67.33**	**-10.00**	**-4327.60**	**844.10**

Notes: The regressed coefficients in the table are only applicable for estimation of residual displacement ratio of trilinear oscillators within the parameter matrix.